JOURNAL OF AIRCRAFT
Vol. 34, No. 5, September–October 1997

Post-Instability Behavior of a Structurally Nonlinear Airfoil in Longitudinal Turbulence

Dominique C. Poirel*
National Defence Headquarters, Ottawa, Ontario K1A 0K2, Canada
and
Stuart J. Price†
McGill University, Montreal, Quebec H3A 2K6, Canada

The effect of longitudinal atmospheric turbulence on the dynamics of an airfoil with a hardening cubic structural nonlinearity in pitch is investigated. The aerodynamics is taken as linear. For the so-called nonexcited case, corresponding to zero turbulence, two distinct regions of dynamic response are obtained. For velocities below the flutter speed, the airfoil response is characterized as a stable equilibrium position; whereas after the onset of flutter, limit cycle oscillations occur. However, three different regions of dynamic behavior are observed when the airfoil is excited by longitudinal turbulence. For the lowest and highest ranges of velocity, the dynamic response is the same as that obtained for the nonexcited case. However, in the middle range of velocities, a new form of dynamic behavior is obtained, where the airfoil response is concentrated about the equilibrium position. The existence of this new region of dynamic behavior is attributed to the parametric nature of the excitation. In addition, for the excited case, flutter occurs at a lower velocity than for the nonexcited case; whereas the onset of limit cycle oscillations occurs at a higher velocity.

Nomenclature

a_h = nondimensional distance between elastic axis and midchord
b = semichord
h, α = airfoil motion in plunge and pitch directions
I_α = airfoil moment of inertia about the elastic axis
K_h, K_α = linear heave and pitch stiffnesses
K_3 = cubic pitch stiffness
k = reduced frequency, $\omega b/U_m$
k_3 = nondimensional cubic pitch stiffness, K_3/K_α
L_{nd} = nondimensional scale of turbulence, L/b
$L(t)$, $M_{ea}(t)$ = lift force and aerodynamic moment about the elastic axis
M = modulus for pseudorandom number generator
m = airfoil mass
r_α = nondimensional radius of gyration
U = total freestream velocity, $U_m + u_g$
$U_{f,nd}$ = nondimensional flutter speed
$U_{m,nd}$ = nondimensional mean freestream velocity, $U_m/b\omega_\alpha$
$U_{1,nd}$, $U_{2,nd}$ = nondimensional bifurcation speeds
u_g, v_g, w_g = gust velocities
x_m, y_m, z_m = mean freestream system of coordinates
x, y, z = body-fixed system of coordinates
x_α = nondimensional distance from elastic axis to c.m.
μ = nondimensional airfoil mass, $m/\rho\pi b^2$
ρ = density of air
σ_g^2 = gust velocity variance
$\sigma_{g,nd}^2$ = nondimensional longitudinal gust velocity variance, $\sigma_g^2/(b\omega_\alpha)^2$
Φ = Wagner's function
ϕ_g = gust velocity power spectral density
ϕ_{wn} = white noise power spectral density
ω = radian frequency
ω_h, ω_α = radian frequencies in plunge and pitch
$'$ = derivative with respect to time

Presented as Paper 96-1341 at the AIAA/ASME/ASCE/AHS/ASC 37th Structures, Structural Dynamics, and Materials Conference, Salt Lake City, UT, April 15–17, 1996; received Aug. 11, 1996; revision received March 22, 1997; accepted for publication April 11, 1997.

*Captain, Directorate Technical Airworthiness. Senior Member AIAA.
†Professor, Department of Mechanical Engineering. Senior Member AIAA.

Introduction

THE deterministic, constant coefficient, two-dimensional, airfoil with structural nonlinearities in attached incompressible flow has been, and still is, a rich source of unexplored nonlinear dynamical behavior. A good review of potential sources of such structural nonlinearities is given by Breitbach.[1] Research on this problem is currently being undertaken at various institutions,[2–5] where a number of interesting phenomena have been predicted. For example, regions of limit cycle oscillations, LCOs, below the main flutter boundary have been predicted, and for certain airfoil parameters the existence of chaotic oscillations was suggested and recently confirmed via calculation of the Lyapunov exponents.[4] However, the system under consideration in these investigations is an idealization of the real problem. One particular idealization is that the airfoil is assumed to be free of any sources of perturbation, which in reality, are always present. From both a practical and theoretical point of view, this raises the question of the presence of random noise.

In the past two decades, physicists have studied the problem of stochastic fluctuations in light of the recent interest and understanding of chaotic behavior and related nonlinear dynamics. They have revised the classical, intuitive reasoning that considers randomness in a system as a secondary effect. In fact, it can no longer be argued that stochastic fluctuations should be averaged, or filtered, out of signals arising from nonlinear deterministic systems. Furthermore, it is now realized that a nonlinear system excited by parametric random noise can produce bifurcation phenomena and organized behavior that have no analog in their deterministic counterparts. These phenomena have been designated as noise-induced tran-

sitions.[6] They are a product of the interplay between stochastic fluctuations and nonlinear dynamics.

The interest of the engineering community in the interaction of random excitations with deterministic chaos and related nonlinear dynamics has been more recent. However, aeroelastic systems offer a potentially important domain of stochastic nonlinear dynamic phenomena. In particular, atmospheric turbulence is a ubiquitous source of random noise. Published work on the effect of atmospheric turbulence on the two-dimensional airfoil has concentrated mainly on the linear problem.[7,8] However, new aircraft technologies are learning to cope and use nonlinear characteristics to their full potential. For example, flight envelopes of the latest generation of fighter aircraft contain pockets of LCOs at dynamic pressures higher than the linear flutter speed.[9–11] Thus, it is crucial to understand the interaction of stochastic excitations and nonlinear dynamics from an aeroelastic perspective. The aim of this paper is to explore and describe some of the effects of atmospheric turbulence on the dynamic response of an airfoil with a structural nonlinearity.

Problem Description

Atmospheric Turbulence Modeling

Atmospheric turbulence models can generally be categorized within two different approaches.[12] The methods associated with a discrete gust representation are usually of a deterministic nature. On the other hand, continuous turbulence methods allow for a stochastic perspective. Hybrid methods also exist and are used in some cases, such as the statistical discrete gust. In the present analysis, the interest lies in the effect of nonlinearities from a dynamics perspective, as opposed to design load requirements. Thus, a continuous stochastic approach is required for the turbulence model.

The theory of isotropic, stochastic, continuous turbulence was pioneered by Taylor and von Kàrmàn (see Ref. 13). In addition to being isotropic, which loosely means that its properties are independent of orientation at any point in space, the atmosphere is usually assumed to be stationary and homogeneous. In general, atmospheric turbulence is considered to be a function of three spatial dimensions and time. However, if a mean freestream velocity U_m is superimposed on this field of fluctuations, u_g, v_g, and w_g, it may be assumed that for a coordinate system attached to the mean velocity (x_m, y_m, z_m, and t), the temporal gradients of turbulent velocity fluctuations are small compared to the spatial gradients; thus, temporal changes can be neglected. This is known as Taylor's hypothesis, or the frozen gust assumption.[14] Since temporal gradients are neglected, a transformation from a spatial to a time system of coordinates is permissible. For example, the longitudinal gust with a mean freestream velocity along the x_m axis gives

$$u_g(x_m, y_m, z_m, t) = u_g(x_m, y_m, z_m) = u_g(x - U_m t, y, z) \quad (1)$$

where x, y, and z form the body-fixed system of coordinates. Hence, at any point fixed on the airfoil, the longitudinal gust is considered as a function of time only.

In two-dimensional flow, the atmospheric turbulence velocity field is composed of vertical and longitudinal components. The vertical component acts as an external forcing function and does not alter fundamentally the low-dimensional dynamics of the otherwise deterministic airfoil response. On the contrary, the longitudinal turbulent field excitation, also known as head-on turbulence, is parametric as it acts on the airspeed. It is in this context that the stochastic system behavior departs from its deterministic counterpart and induces new bifurcation phenomena. In this paper, only the effect of longitudinal atmospheric turbulence is considered.

Further assumptions of continuous atmospheric turbulence, as traditionally applied to aircraft, are a Gaussian distribution and spanwise uniformity. In this paper, the latter is implicitly assumed because of the two-dimensional nature of the airfoil. Changes along the vertical axis are also neglected. In addition, chordwise uniformity is assumed to facilitate the aerodynamic modeling, as discussed later in this paper. Subsequently to Eq. (1), the uniformity assumption permits the gust to be expressed in a body-fixed coordinate system as

$$u_g(x - U_m t, y, z) = u_g(t) \quad (2)$$

The spectral content of turbulence can be provided by either the von Kàrmàn or Dryden models, which are presently the two most widely accepted models. The Dryden model is used in the work presented here, since it is easier to handle mathematically. The one-sided PSD Dryden longitudinal gust representation is given as[15]

$$\phi_g(\omega) = \sigma_g^2 2(L/\pi U_m)/[1 + (L\omega/U_m)^2] \quad (3)$$

and is presented in nondimensional form in Fig. 1 for the particular scales of turbulence considered in this paper. It can be shown that the scale of turbulence L, divided by the mean freestream velocity U_m, is equal to the correlation time of the random excitation. This representation is known as Ornstein–Uhlenbech noise in physics literature.[6]

Airfoil Structural Modeling

The airfoil is modeled as a typical section with degrees of freedom in pitch and heave. Structural flexibility is provided by torsional and translational springs. A hardening cubic representation of the torsional spring is considered, this is the only source of nonlinearity. Other nonlinearities, such as the geometric terms have been neglected; thus, oscillations are limited to small amplitudes. Structural damping is also neglected. The structural equations, given for example by Fung,[16] and modified to include the nonlinearity, are

$$\begin{aligned} mh'' + mx_\alpha b\alpha'' + K_h h &= L(t) \\ (I_\alpha + mx_\alpha^2 b^2)\alpha'' + mx_\alpha bh'' + K_\alpha \alpha + K_3\alpha^3 &= M_{ea}(t) \end{aligned} \quad (4)$$

Aerodynamic Modeling

Only attached flow conditions with small amplitude oscillations are considered; hence, the aerodynamics are linear. The unsteady aerodynamics accounting for memory effects are modeled, assuming incompressible inviscid flow, via Duhamel's integral and the two-state representation of Wagner's function.[16–18] This is usually referred to as the arbitrary-motion

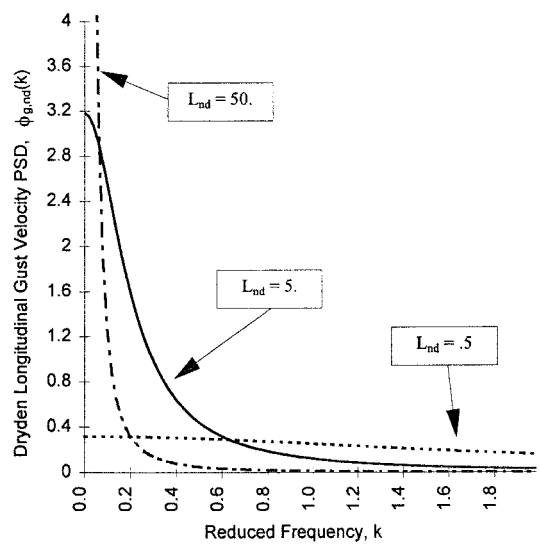

Fig. 1 Nondimensional PSD of the Dryden longitudinal gust for different scales of turbulence; closed-form solution for $\sigma^2_{gnd} = 1.0$.

theory. Classically, it considers motion in the structural degrees of freedom only, where the downwash at the three-quarter-chord position represents the effective downwash on the airfoil.[16]

In this paper, the arbitrary-motion theory is extended for the case of a random time-varying airspeed, based on the work of Van der Wall and Leishman.[17] They show that the arbitrary-motion theory compares very well with Isaacs' theory,[19] for the case of periodic fore–aft movements of an airfoil, along with pitch and heave oscillations. In fact, the only difference appears to be attributable to the limited number of states used in the approximate representation of Wagner's function. Note, that Isaacs[19] considered only periodic fore–aft and pitch oscillations. Isaacs' theory[19] was generalized by Van der Wall[18] to include heave motion as well, and can be considered exact for the preceding fluid assumptions.

It is important to note that fore–aft movement of an airfoil in a uniform stream is not physically the same as fluctuations of the freestream velocity. In the first case, which is treated by Isaacs,[19] the airflow is uniform along the chord. On the other hand, a chordwise velocity gradient exists for a varying freestream velocity, which is the case investigated in this paper. This difference affects both the noncirculatory force and moment, as well as the bound vorticity of the circulatory terms. However, the free vortex sheet in the airfoil wake is the same in both cases. Van der Wall and Leishman[17] showed that fore–aft movement aerodynamics is an approximation of the unsteady freestream problem, which is valid only for small frequencies. The chordwise uniformity of the airflow assumption is considered here and is extended to the case of random fluctuations. This is supported by the atmospheric turbulence velocity spectrum being concentrated in the low-frequency range. It is thus assumed that the aerodynamic forces induced by random variations of the freestream velocity, and accounting for arbitrary pitch and heave motions, can be accurately modeled by the following:

$$
\begin{aligned}
-L(t) &= -\pi\rho b^2(h'' + U\alpha' + U'\alpha - ba_h\alpha'') \\
&\quad - 2\pi\rho bU\left[\Omega_{3/4}(t)\Phi(0) - \int_0^t \Omega_{3/4}(s)\,\frac{\mathrm{d}\Phi(t-s)}{\mathrm{d}s}\,\mathrm{d}s\right] \\
M_{ea}(t) &= \pi\rho b^2\left[ba_h h'' - b\left(\frac{1}{2} - a_h\right)U\alpha'\right. \\
&\quad \left. - b\left(\frac{1}{2} - a_h\right)U'\alpha - b^2\left(a_h^2 + \frac{1}{8}\right)\alpha''\right] + 2\pi\rho b^2 \\
&\quad \times \left(a_h + \frac{1}{2}\right)U\left[\Omega_{3/4}(t)\Phi(0) - \int_0^t \Omega_{3/4}(s)\,\frac{\mathrm{d}\Phi(t-s)}{\mathrm{d}s}\,\mathrm{d}s\right]
\end{aligned}
\tag{5}
$$

where $\Omega_{3/4}(t) = h' + U\alpha + b(1/2 - a_h)\alpha'$ and $\Phi(t) = 1 - 0.165\exp(-0.0455U_m t/b) - 0.335\exp(-0.3U_m t/b)$.

The first terms in the lift and moment expressions represent the noncirculatory forces, associated with fluid inertia. The circulatory forces, given by the second terms, model the effect of the bound vorticity and the shed wake, convecting downstream at velocity $U(t) = U_m + u_g(t)$. Note, that the integral term given in Refs. 17 and 18 has been integrated by parts leading to Eq. (5).

Numerical Simulation

Time-Domain Integration

The numerical solution is based on a fourth-order Runge–Kutta algorithm. The equations of motion must first be expressed in state-space form, giving a seventh-order system. Four states represent the structural degrees of freedom. Two of the other states are associated with the lag terms of the aerodynamics, which appear after reformulation of the integral in the circulatory force. This leads to an additional second-order ordinary differential equation (ODE), given by

$$
\int_0^t \Omega_{3/4}(s)\,\frac{\mathrm{d}\Phi(t-s)}{\mathrm{d}s}\,\mathrm{d}s = -\left(0.0455 \times \frac{0.3}{2}\right)\frac{U_{m^2}}{b}Z(t) - (0.165 \times 0.0455 + 0.335 \times 0.3)\,\frac{U_m}{b}Z'(t) \tag{6}
$$

where

$$
Z''(t) + (0.0455 + 0.3)(U_m/b)Z'(t) + (0.0455 \times 0.3)(U_m/b)^2 Z(t) = \Omega_{3/4}(t)
$$

The final state of the seventh-order system models the Dryden longitudinal gust, whose PSD is given by Eq. (3). In the time domain, it is transformed as

$$
u_g'(t) = -u_g(t)U_m/L + \sigma_g(2U_m/\pi L\phi_{wn})^{1/2}G_{wn}(t) \tag{7}
$$

where G_{wn} is Gaussian white noise, whose intensity is defined by a single-sided PSD of magnitude one; i.e., $\phi_{wn} = 1$. The airfoil system, modeled by a set of parametrically excited stochastic nonlinear differential equations

$$
[M]\{\boldsymbol{q}''\} + [D(t)]\{\boldsymbol{q}'\} + [K(t)]\{\boldsymbol{q}\} + [K_3]\{\boldsymbol{q}^3\} = \{\boldsymbol{0}\} \tag{8}
$$

where $\{\boldsymbol{q}\} = \{\alpha, h, Z\}^T$ can then be combined with Eq. (7). The damping and stiffness matrices $[D(t)]$ and $[K(t)]$, respectively, are time dependent because of the longitudinal turbulence in the aerodynamic terms. The cubic stiffness matrix $[K_3]$, remains constant, however, because the nonlinearity is purely structural.

Finally, in state–space form, the seventh-order system of stochastic differential equations may be expressed as

$$
\{\boldsymbol{x}'\} = [A(t)]\{\boldsymbol{x}\} + [A_3]\{\boldsymbol{x}^3\} + [B]\{\boldsymbol{g}(t)\} \tag{9}
$$

where $\{\boldsymbol{x}\} = \{\alpha, h, \alpha', h', Z, Z', u_g\}^T$, $\{\boldsymbol{g}(t)\} = \{0, 0, 0, 0, 0, 0, G_{wn}(t)\}^T$, and $[A(t)]$, $[A_3]$ and $[B]$ are matrices whose individual terms are not given here for the sake of brevity. It is, however, relevant to note that $[A(t)]$ contains quadratic colored noise terms because of the presence of $U(t)^2$.

White Noise and Random Number Generation

The Gaussian white noise is generated at each time step of the integration based on the Box–Muller algorithm.[20] It takes the form

$$
G_{wn}(t) = [-2(\phi_{wn}\pi/\Delta t)\ell n\, u_1]^{1/2}\cos 2\pi u_2 \tag{10}
$$

The terms u_1 and u_2 are uniformly distributed pseudorandom numbers on the interval (0,1], obtained from an International Mathematical and Statistical Library (IMSL) subroutine,[21] based on a multiplicative congruential generator. It is internally programmed in machine language; whereas a higher level programming would restrict the properties of the generated sequence[22] too much. It produces the sequence of nonnegative integers

$$
a_i = Ca_{i-1} \bmod(M), \qquad i = 1, 2, 3, \ldots \tag{11}
$$

The sequence is initiated with a seed, a_0, chosen between 1 and the maximum value that can be generated by the generator. The maximum value of the sequence is called the period of the generator and is determined by the combination of the modulus M and multiplier C. An appropriate choice of M and C gives a maximum period equal to the modulus, thus providing a uniform distribution within the interval (1,M]. The distribution is then normalized by dividing each generated number by the modulus. The bigger the modulus, the denser the

points are in the unit interval (0,1]; in the limit the distribution becomes continuous. Other desirable properties of this method are related to the independence between numbers, and also between the sequence of numbers. These have been shown to be a potential problem for the congruential generator if the multiplier–modulus combination is not chosen carefully.[23] Reference 23 provides a detailed analysis of different multipliers used in conjunction with the multiplicative congruential generator of modulus $2^{31} - 1$. A battery of statistical tests is applied to different sequences of pseudorandom numbers, and the best multipliers are determined. In this paper, M is taken as $2^{31} - 1$, and C is chosen as 950706376, which is considered the best multiplier.[23] This multiplier also ensures a period equal to the modulus.

The same multiplier–modulus combination will always give the same sequence for similar seeds. Thus, this is obviously a deterministic process, and is the reason why the numbers are described as pseudorandom as opposed to being truly random. The fact that the sequence of numbers originates from a deterministic process is in itself not relevant. It can be argued that randomness is a way to account for variations that cannot be controlled, or which we choose not to control. In this light, randomness may not have any physical basis, but this is a philosophical question. What counts is that the sequence of numbers possesses some basic statistical properties, and that the solution of the problem is independent of the origin of these random numbers. This last point will be addressed in the next subsection.

Solution Methodology and Validation

Results have been generated using a fourth-order Runge–Kutta numerical integration scheme. Bearing in mind the stochastic nature of the process, special attention is given to the size of the time step and the number of iterations. Also, we are interested in the steady-state response only, the time required for the initial transient response to die out is also of interest. The factors that determine the magnitude of the time step are numerical stability and noise correlation time, L/U_m. Accordingly, the time step is taken as the smallest of either 1/128 of the lowest uncoupled natural frequency of the airfoil or 1/5 of the noise correlation time. A very large number of iterations is necessary to ensure a smooth probability density distribution (PDD). This is particularly important when examining the dynamics of the system, as opposed to a loads analysis. For example, the variance is much less sensitive to the sample size in the PDD. For the work presented in this paper, 4×10^6 to 8×10^6 iterations were used. With regard to the transient time, it is first approximated by the noise correlation time, the gust being modeled by a linear first-order ODE, the transient time is determined analytically, and by a visual interpretation of the deterministic response. This is then verified for the stochastic case by comparing statistical and probabilistic measures for different sample time lengths.

Validation of the results presented in the next section is approached from different levels. One validation is based on a comparison of some test cases with Houbolt's implicit finite difference method,[24] which, in principle, is more robust. For the cases tested, both numerical integration schemes gave indistinguishable results. Further validation was obtained by investigating the sensitivity of the results to the time step and sample time length. Finally, the randomness of the pseudorandom number sequence was examined to ensure independence of the results with respect to the generator. For the same modulus, a multiplier of 16,807 was tested in comparison with the best multiplier used throughout this paper; no significant differences were noted. In addition, a shuffled version of the pseudorandom number sequence was also tested, and again, no difference in the system dynamics was noticed.

Figures 2 and 3 present results giving a validation of the spectral content, Gaussian distribution, and intensity of the numerically generated gust. It is observed that the PDD is nearly

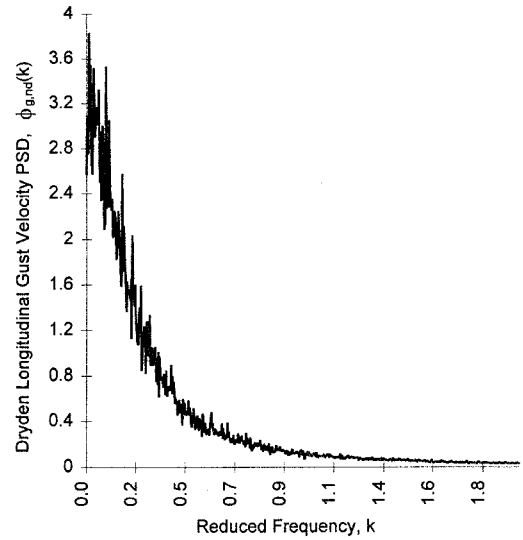

Fig. 2 Numerical solution of longitudinal Dryden gust PSD for $\sigma^2_{g,nd} = 1.0$ and $L_{nd} = 5.0$.

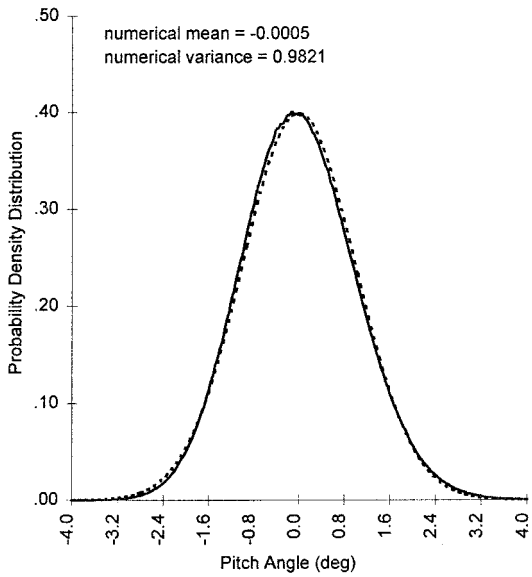

Fig. 3 Comparison of the numerical solution with the true Gaussian curve of the longitudinal Dryden gust PDD for $\sigma^2_{g,nd} = 1.0$ and $L_{nd} = 5.0$.

Gaussian in comparison with a theoretical curve. Furthermore, the PSD and variance obtained numerically closely match the closed-form expression represented by Fig. 1.

Numerical Results and Discussion

Before presenting results showing the effect of longitudinal atmospheric turbulence on the flutter and postflutter response, the dynamics of the deterministic (nonexcited) airfoil will be discussed. The cases presented are for an airfoil with the following nondimensional parameters: $k_3 = 400$, $\omega_h/\omega_\alpha = 0.6325$, $x_\alpha = 0.25$, $r_\alpha = 0.5$, $\mu = 100$, and $a_h = -0.5$.

For comparison purposes, Fig. 4 presents bifurcation diagrams of the airfoil response as the airspeed is increased for both the nonexcited and excited cases. At this point, however, we shall limit our attention to the nonexcited case. The vertical axis shows both the traditional amplitude of oscillation and the variance of the airfoil pitch motion. For low airspeeds, the bifurcation diagram indicates a stable equilibrium point, which becomes unstable for airspeeds $U_{m,nd} \geq 4.31$. The point $U_{f,nd} = 4.31$ is the flutter speed, and corresponds to a supercritical Hopf-bifurcation, because the dynamics for higher airspeeds is

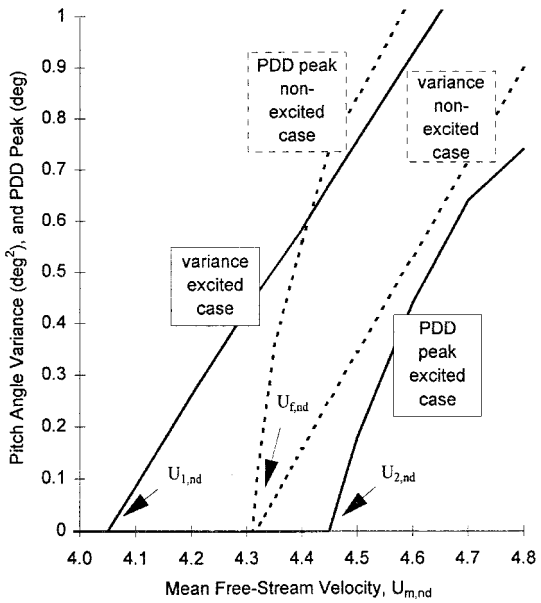

Fig. 4 Bifurcation diagram of the airfoil response for the excited and nonexcited cases; $\sigma^2_{g,nd} = 1.0$ and $L_{nd} = 5.0$.

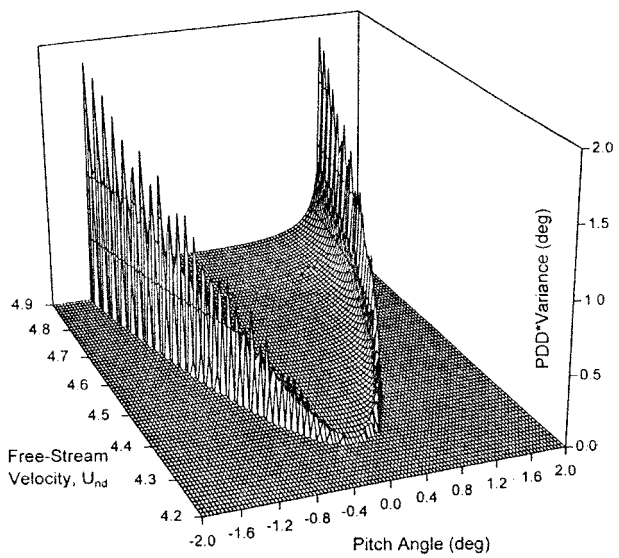

Fig. 5 Bifurcation diagram of the airfoil PDD response for the nonexcited case.

an unstable equilibrium coinciding with a stable limit cycle oscillation (LCO). The flutter speed and Hopf-bifurcation (LCO onset) are uniquely determined by either the amplitude of the pitch oscillation or its variance. In general terms, a bifurcation is defined as being where there is a qualitative change in the topological structure of the dynamic behavior.[25] In a deterministic system, this definition corresponds exactly to the point in parameter space where one of the Lyapunov exponents vanishes, and thus, it is associated with a critical slowdown of the dynamics. For our case, linearization of the system about the fixed point gives a complex conjugate pair of eigenvalues, whose real parts go to zero at the flutter speed. Although not presented here, it was found that in the vicinity of the bifurcation point, the LCO reduced frequency is approximately 0.18.

Since our fundamental interest is in the stochastic (randomly excited) case, it is relevant to describe the dynamics of the deterministic system in terms of a PDD. Figure 5 presents the deterministic bifurcation scenario from this perspective. Note, that the vertical axis shows the probability density multiplied by the variance of the response. This representation shows two qualitatively different regions of dynamical behavior; before and after the Hopf-bifurcation. Prior to the Hopf-bifurcation, the response is characterized by a flat distribution, which indicates zero variance or no dynamics. Remember that the vertical axis is the PDD multiplied by the variance. For a pure PDD plot, we would have a Dirac delta function centered at zero pitch angle, but in this region the variance is zero. The LCO response after the Hopf-bifurcation is characterized by a crater-like shape, the peaks of which correspond to the most probable value that the pitch angle will take during the motion, and thus, to the amplitude of oscillation. Hence, the variance and the location of the peaks of the PDD will be the two main measures for the system dynamics.

We now discuss the excited case. Figure 6 shows the PDD multiplied by the variance of the stochastic pitch response for a range of mean freestream velocities. It is the equivalent of Fig. 5, but for the excited system. For the results of Fig. 6, the gust variance is $\sigma^2_{g,nd} = 1.0$, and the scale of turbulence is $L_{nd} = 5.0$, as employed for the results of Figs. 2 and 3. It is apparent that there are now three distinct regions of qualitatively different dynamic behavior, separated by two critical airspeeds: $U_{1,nd} \approx 4.05$ and $U_{2,nd} \approx 4.45$. This suggests that the response goes through two bifurcations instead of one. The first region, for velocities $\leq U_{1,nd}$, is characterized by a flat distribution, indicating no dynamics. It is only in the third region, for velocities $\geq U_{2,nd}$, that the response demonstrates fully developed periodic oscillations (Fig. 7d), and we recognize the double-peaked crater-like shape of the PDD representation that characterizes the LCO motion. The pitch angles at the peaks of the PDD are analogous to the amplitude of the LCO motion of the deterministic case. The second region, between $U_{1,nd}$ and $U_{2,nd}$, is denoted by a single peak with some diffusion about its mean, which occurs at zero pitch angle. Therefore, the most probable value that the pitch angle will take during this motion is zero. From the perspective of a time history, which is perhaps a more familiar conceptual tool, dynamical behavior is seen, but no fully developed oscillations are observed (Fig. 7c). The results shown in Fig. 7 give a detailed representation and comparison of the dynamics between the second and third regions in terms of PDDs, time histories, and PSDs. The only clear distinction occurs in the PDD representation. However, as mentioned earlier, the time history plots give an indication of the overall behavior. The PSDs of the pitch angle, Figs. 7e and 7f, indicate the presence of a second frequency peak, in addition to the LCO frequency peak, which seems to correspond to the natural frequency of the stable mode, i.e., mode 2, of the linear system.

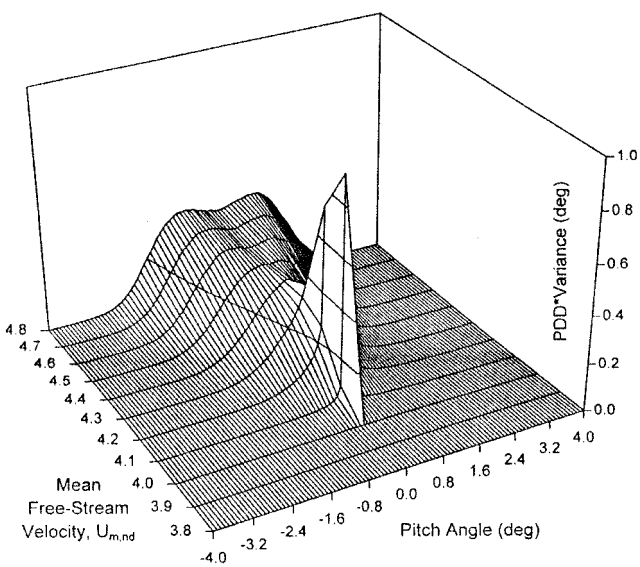

Fig. 6 Bifurcation diagram of the airfoil PDD response for the excited case; $\sigma^2_{g,nd} = 1.0$ and $L_{nd} = 5.0$.

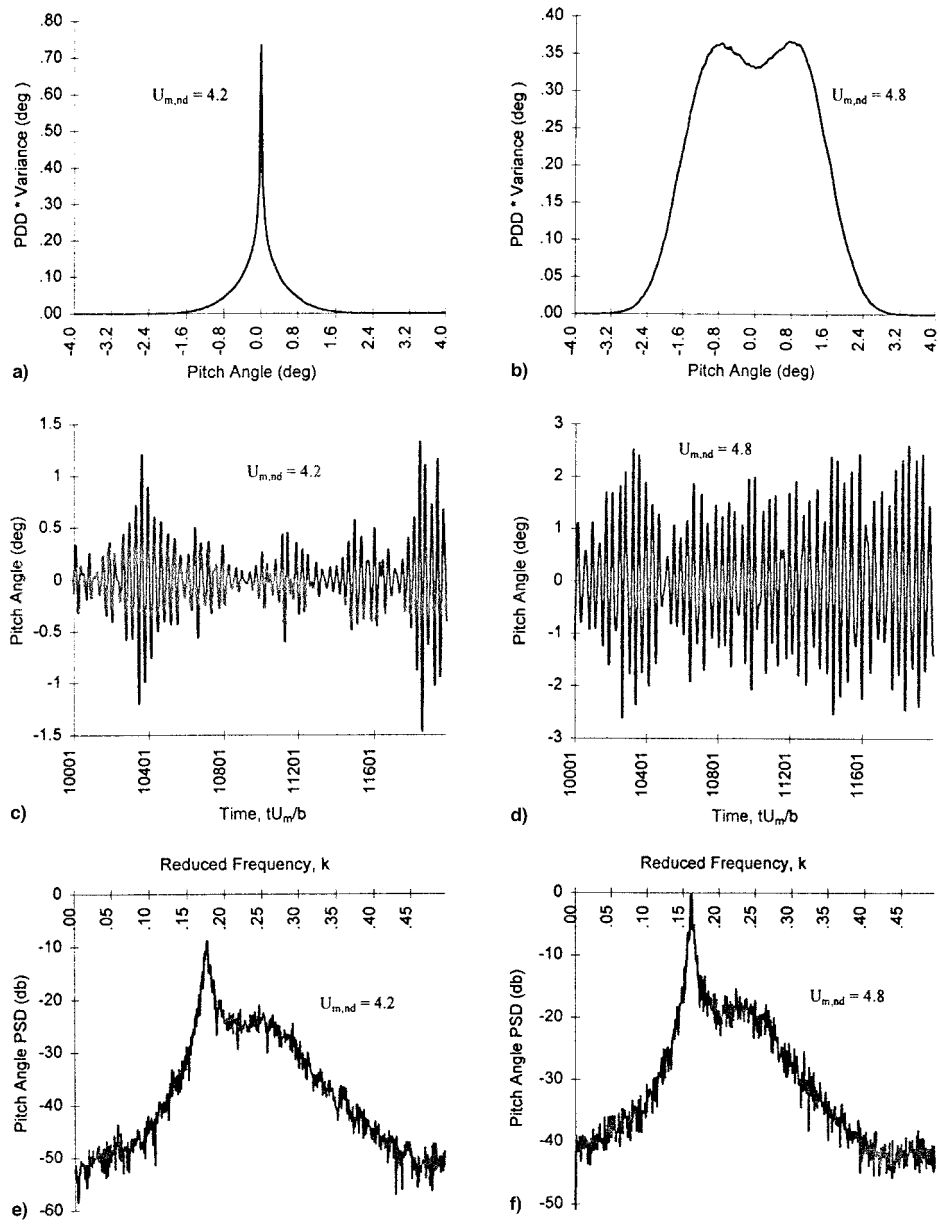

Fig. 7 Detailed comparison of the dynamics in the second and third regions: a), c), and e) $U_{m,nd} = 4.2$; b), d), and f) $U_{m,nd} = 4.8$. a) and b) PDDs, c) and d) time histories, and e) and f) PSDs.

A second observation is that the flutter speed and Hopf-bifurcation are apparently no longer coincident. It is suggested that $U_{1,nd}$ defines the stochastic flutter speed, as the equilibrium state becomes dynamically unstable at this velocity. Flutter bears its origin from a linear approach, and thus, can be observed with a linearized system. Because of the stochastic nature of the parametrically excited system, it is difficult to pinpoint exactly the point of instability of the linear airfoil using a numerical time integration method. This is because the closer we are to the instability, the lower the damping of the slow variable; thus, locally exceeding the maximum value permitted by the simulation, even though global statistical measures such as mean and variance are within an acceptable range. However, the flutter point can still be determined within an acceptable margin of error. To that extent, numerical solutions of the system with different magnitudes of the nonlinear stiffness coefficient, $50 \leq k_3 \leq 800$, gave exactly the same flutter speed, confirming that this is a linear phenomenon.

The definition of the stochastic Hopf-bifurcation point is somewhat more ambiguous and leaves room for interpretation. Although the spectrum of Lyapunov exponents has not been calculated for the second bifurcation, intuitively it is suggested that this second topological change in the dynamics is not associated with a vanishing of the exponents or a critical slowdown of the dynamics. This is contrary to deterministic bifurcation phenomenon, and is purely a product of the interaction between the stochastic and nonlinear natures of the system. In the recent and quickly evolving area of stochastic nonlinear dynamical systems, this bifurcation type is called a P-bifurcation (P for phenomenological).[26] The first bifurcation is termed a D-bifurcation (D for dynamical). For the present case, it is argued that the P-bifurcation represents the stochastic Hopf-bifurcation and occurs at $U_{2,nd}$, i.e., where the PDD changes from being single to double peaked, and also where fully developed periodic oscillations start to appear in the time history.

A third observation concerns the exact location of the two bifurcation airspeeds. This is best seen from the results of Fig. 4, where the vertical axis shows the variance and most probable value of the pitch state. For this particular set of parameters, interpolation of the variance results suggests the stochastic flutter point to be at $U_{1,nd} = 4.05$, while the most probable value results suggest that the stochastic Hopf-bifurcation occurs at $U_{2,nd} = 4.45$. Also presented in Fig. 4 for

comparison is the nonexcited deterministic case. We see that, compared with the nonexcited case, the effect of the longitudinal random gust is to advance the flutter speed and to postpone the onset of the LCO. Advancement of the flutter point can be explained, in part, because of the quadratic airspeed term. In effect, the longitudinal gust increases the average magnitude of the dynamic pressure, as defined by $\rho\bar{U}^2/2$ or $\rho(U_m^2 + u_g^2)/2$, so that the dynamic pressure term associated with the mean airspeed at which flutter occurs is lower than for the nonexcited case. The presence of the random component in the linear airspeed term also influences the location of the flutter point, but may advance or retard it (see Refs. 8 and 27), where the effect of atmospheric turbulence on the aeroelastic response of a linear rotor blade was studied. In the work of Refs. 8 and 27, quasisteady aerodynamics were employed, and the effect of the quadratic noise term was neglected; also white noise was assumed. Using Ito's calculus to obtain a closed-form solution, it was found that linear noise can either advance or postpone the flutter point.[8,27]

The effects of gust intensity and frequency content were investigated, and some results are presented in Fig. 8, where the two bifurcation airspeeds are plotted as a function of gust variance for three different scales of turbulence. Evidently, the zero gust variance point corresponds to the deterministic case; thus, we recognize the unique flutter and Hopf-bifurcation airspeeds, $U_{f,nd} = 4.31$. As the variance is increased, the region of single peak PDD becomes larger for all three cases. However, the second bifurcation point, $U_{2,nd}$, seems to depart from the nonexcited case at a lower rate than the first bifurcation. Hence, further enlargement of this region is mainly because of the advancement of the flutter speed, $U_{1,nd}$. Again, it is proposed that the noise component of the quadratic airspeed term explains this behavior.

The effect of scale of turbulence, which is a measure of the frequency content, is perhaps more interesting. For equivalent gust variances, the two bifurcation airspeeds approach each other as the bandwidth of the gust is increased. This is explained by noting that the effective portion of the excitation on the system, which is defined by the range of natural frequencies or time scales of the deterministic airfoil relative to the gust bandwidth, decreases for a larger total bandwidth. By referring to Fig. 1, we see that the area under the PSD curves for reduced frequencies lower than 0.18, which is the LCO frequency, decreases for smaller scales of turbulence.

The following discussion perhaps brings a more practical perspective to the behavior and significance of the single-peak region. This region has no analog in the deterministic case, as opposed to the two extreme regions. It cannot be approximated

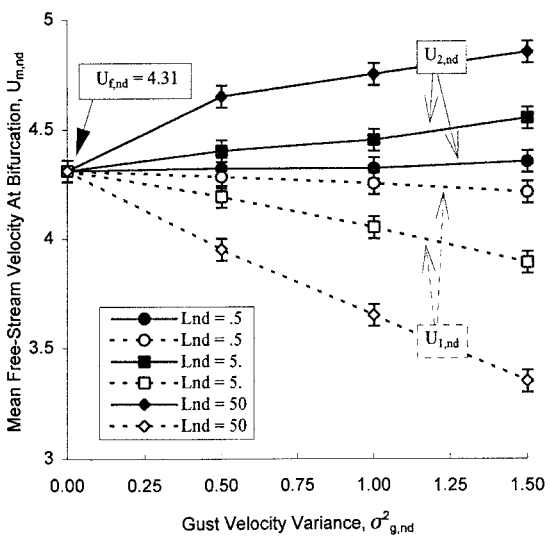

Fig. 8 Bifurcation diagram of the mean freestream velocities as a function of the gust variance for three scales of turbulence.

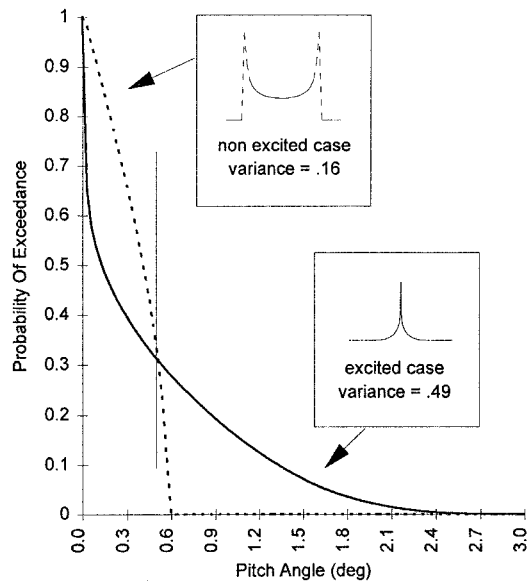

Fig. 9 Probability of exceedance as a function of airfoil pitch angle.

by either an equilibrium point, nor a limit cycle oscillation. We mentioned earlier, that although dynamical behavior is observed between $U_{1,nd}$ and $U_{2,nd}$, the most probable value that the pitch (or heave) variable takes during the motion is zero. This has some significance in terms of structural fatigue considerations. In Fig. 9, a comparison is shown between the probability of exceedance of the pitch angle (the probability that the airfoil pitch exceeds a specific value) for the deterministic and stochastic cases for the same mean freestream velocity. The probability of exceedance is related to the frequency of exceedance, and provides some indication of the susceptibility of the structure to fatigue deterioration. In this example, the variance of the pitch response for the excited case is roughly three times larger than for the nonexcited case. This suggests that structural fatigue could be much more problematic in the presence of a longitudinal gust than without it. However, since most of the dynamics are concentrated about the zero pitch angle, only a small fraction of the motion has an impact on fatigue. This is contrary to the nonexcited case, where the dynamics are concentrated about a nonzero pitch amplitude. If, for example, a pitch angle of 0.5 deg is defined as the critical point for fatigue considerations, the example of Fig. 9 shows that the probability of the pitch exceeding this critical angle is higher for the nonexcited case than it is for the gust-excited airfoil. The conclusion that follows is therefore in contradiction to the one strictly based on response variance.

Conclusions

The addition of the effect of longitudinal atmospheric turbulence on the aeroelastic modeling and analysis of the nonlinear airfoil not only sheds a more realistic light on the dynamical behavior, but also leads to the observation of phenomenon not present in the purely deterministic system. For the flutter/Hopf-bifurcation of a stiffening cubic torsional spring, the following points have been noted:

1) Three regions of topologically different dynamic behavior are observed instead of two. The two extreme regions have their analog in the deterministic case, i.e., an equilibrium point and a limit cycle oscillation. The middle region is purely a result of the combined nonlinear and stochastic nature of the system.

2) Because there are now three different regions of dynamic behavior, there are two bifurcation points. The first one is the stochastic flutter speed, and the second one corresponds to the stochastic Hopf-bifurcation point or to the onset of the stochastic LCO.

3) For the case considered in this paper, the flutter speed is advanced by the presence of the random gust, while the Hopf-bifurcation is postponed. Hence, it appears that the longitudinal turbulence may lower the dynamic pressure associated with the mean airspeed at which flutter occurs.

4) The frequency content of the gust excitation, expressed via the scale of turbulence, has the effect of bringing together the two bifurcation airspeeds as the bandwidth is increased.

5) The effect of gust intensity, or variance, is to separate the two bifurcation airspeeds. However, the Hopf-bifurcation point tends to depart from the nonexcited value at a lower rate than the flutter speed does.

6) From a more practical perspective, the presence of longitudinal atmospheric turbulence may alleviate the problem of structural fatigue by forcing the airfoil dynamics to be concentrated in a region about the zero pitch angle, and to be of small amplitude.

It is emphasized that these conclusions are related to longitudinal gust excitation only. Its effect is parametric as it acts via the airspeed. However, in a real environment, the other gust components, vertical and lateral, are also present. They act as external forcing functions, and thus, should not alter the stability or flutter speed of the system. Their influence will, however, be felt on the nonlinear response characteristics. The previous conclusions must therefore be verified when the presence of a vertical gust acting on the two-dimensional airfoil is also accounted for. In addition, for the parametric case, Lyapunov exponents should be calculated numerically in the vicinity of the two bifurcations.

Acknowledgments

The authors gratefully acknowledge the support of the Department of National Defence, the Institute for Aerospace Research, and the Natural Sciences and Engineering Research Council of Canada.

References

[1]Brietbach, E., "Effect of Structural Nonlinearities on Aircraft Vibration and Flutter," 45th Structures and Materials AGARD Panel Meeting, AGARD Rept. 665, 1977.

[2]Price, S. J., Lee, B. H. K., and Alighanbari, H., "Postinstability Behavior of a Two-Dimensional Airfoil with a Structural Nonlinearity," *Journal of Aircraft*, Vol. 31, No. 6, 1994, pp. 1395–1401.

[3]Price, S. J., Alighanbari, H., and Lee, B. H. K., "The Aeroelastic Response of a Two-Dimensional Airfoil with Bilinear and Cubic Structural Nonlinearities," *Journal of Fluids and Structures*, Vol. 9, No. 2, 1995, pp. 175–194.

[4]Alighanbari, H., and Price, S. J., "The Post-Hopf-Bifurcation Response of an Airfoil in Incompressible Two-Dimensional Flow," *Nonlinear Dynamics*, Vol. 10, 1996, pp. 381–400.

[5]Liu J.-K., and Zhao L.-C., "Bifurcation Analysis of Airfoils in Incompressible Flow," *Journal of Sound and Vibration*, Vol. 154, No. 1, 1992, pp. 117–124.

[6]Horsthemke, W., and Lefever, R., *Noise-Induced Transitions; Theory and Applications in Physics, Chemistry and Biology*, Springer–Verlag, Berlin, 1984.

[7]Tang, D. M., and Dowell, E. H., "Response of a Nonrotating Rotor Blade to Lateral Turbulence—Part I," *Journal of Aircraft*, Vol. 32, No. 1, 1995, pp. 145–153.

[8]Fuh, J. S., Hong, C. Y. R., Lin, Y. K., and Prussing, J. E., "Coupled Flap-Torsional Response of a Rotor Blade in Forward Flight Due to Atmospheric Turbulence Excitations," *Journal of the American Helicopter Society*, Vol. 28, No. 3, 1993, pp. 3–12.

[9]Lee, B. H. K., and Tron, A., "Effects of Structural Nonlinearities on Flutter Characteristics of the CF-18 Aircraft," *Journal of Aircraft*, Vol. 26, No. 8, 1989, pp. 781–786.

[10]Trame, L. W., Williams, L. E., and Yurkovich, R. N., "Active Aeroelastic Oscillation Control on the F/A-18 Aircraft," *AIAA Guidance, Navigation, and Control Conference* (Snowmass, CO), AIAA, New York, 1985, pp. 94–104.

[11]Meijerm, J. J., and Cunningham, A. M., Jr., "Development of a Method to Predict Transonic Limit Cycle Oscillation Characteristics of Fighter Aircraft," AGARD Specialist's Meeting on Transonic Unsteady Aerodynamics and Aeroelasticity, San Diego, CA, 1991 (Paper 23).

[12]Barnes, T. J., "Overview of the Activities of the ad hoc Committee of International Gust Specialists," AGARD-R-798, 1994.

[13]Houbolt, J. C., Steiner, R., and Pratt, K. G., "Dynamic Response of Airplanes to Atmospheric Turbulence Including Flight Data on Input and Response," NASA TR R-199, June 1964.

[14]Costello, M., Prasad, J. V. R., Schrage, D. P., and Gaonker, G. H., "Some Issues on Modelling Atmospheric Turbulence Experienced by Helicopter Rotor Blades," *Journal of the American Helicopter Society*, Vol. 37, No. 2, 1992, pp. 71–75.

[15]Hoblit, F. M., *Gust Loads on Aircraft: Concepts and Applications*, AIAA Education Series, AIAA, Washington, DC, 1988.

[16]Fung, Y. C., *An Introduction to the Theory of Aeroelasticity*, Wiley, New York, 1955.

[17]Van der Wall, B. G., and Leishman, J. G., "On the Influence of Time-Varying Flow Velocity on Unsteady Aerodynamics," *Journal of the American Helicopter Society*, Vol. 39, No. 4, 1994, pp. 25–36.

[18]Van der Wall, B. G., "The Influence of Variable Flow Velocity on Unsteady Airfoil Behavior," DLR, German Aerospace Research Establishment, DLR-FB 92-22, Feb. 1992.

[19]Isaacs, R., "Airfoil Theory for Flows of Variable Velocity," *Journal of the Aeronautical Sciences*, Vol. 13, No. 4, 1945, pp. 113–117.

[20]Sancho, J. M., San Miguel, M., Katz, S. L., and Gunton, J. D., "Analytical and Numerical Studies of Multiplicative Noise," *Physical Review A, General Physics*, Vol. 26, No. 3, 1982, pp. 1589–1609.

[21]"Fortran Subroutines for Statistical Analysis," International Mathematical and Statistical Library, Houston, TX, 1987.

[22]Press, W. H., Flannery, B. P., Teukolsky, S. A., and Vetterling, W. T., *Numerical Recipes, The Art of Scientific Computing*, Cambridge Univ. Press, Cambridge, England, UK, 1986.

[23]Fishman, G. S., and Moore, L. R., "An Exhaustive Analysis of Multiplicative Congruential Random Number Generators with Modulus $2^{31}-1$," *SIAM Journal on Scientific and Statistical Computing*, Vol. 7, No. 1, 1986, pp. 24–45.

[24]Houbolt, J. C., "A Recurrence Matrix Solution for the Dynamic Response of Elastic Aircraft," *Journal of the Aeronautical Sciences*, Vol. 17, No. 9, 1950, pp. 540–550.

[25]Argyris, J., Faust, G., and Haase, M., "An Exploration of Chaos—An Introduction for Natural Scientists and Engineers," *Texts on Computational Mechanics*, Vol. 7, North-Holland, Amsterdam, 1994.

[26]Arnold, L., Jones, C., Mischaikow, K., and Raugel, G., *Dynamical Systems, Lectures Given at the 2nd Session of the Centro Internazionale Matematico Estivo*, Springer–Verlag, Berlin, 1995.

[27]Prussing, J. E., and Lin, Y. K., "A Closed-Form Analysis of Rotor Blade Flap-Lag Stability in Hover and Low-Speed Forward Flight in Turbulent Flow," *Journal of the American Helicopter Society*, Vol. 28, No. 3, 1983, pp. 42–46.